Localization of a matter wave packet in a disordered potential

M. Piraud[1], P. Lugan[1,2], P. Bouyer[1], A. Aspect[1], and L. Sanchez-Palencia[1]
[1] *Laboratoire Charles Fabry de l'Institut d'Optique, CNRS and Univ. Paris-Sud, Campus Polytechnique, RD 128, F-91127 Palaiseau cedex, France*
[2] *Physikalisches Institut, Albert-Ludwigs-Universität, Hermann-Herder-Str. 3, D-79104 Freiburg, Germany*
(Dated: March 8, 2011)

We theoretically study the Anderson localization of a matter wave packet in a one-dimensional disordered potential. We develop an analytical model which includes the initial phase-space density of the matter wave and the spectral broadening induced by the disorder. Our approach predicts a behavior of the localized density profile significantly more complex than a simple exponential decay. These results are confirmed by large-scale and long-time numerical calculations. They shed new light on recent experiments with ultracold atoms and may impact their analysis.

PACS numbers: 05.60.Gg, 72.15.Rn, 67.85.-d, 03.75.-b

The field of Anderson localization (AL) is attracting considerable attention and produced landmark results in the recent years [1]. In this respect, quantum gases stimulate intensive experimental and theoretical research. On one hand, they offer unprecedented control of their parameters, and novel measurement tools [2], which, for instance, paved the way to the direct observation of one-dimensional (1D) AL of matter waves [3, 4]. On the other hand, they sustain original effects, which require special analysis in its own right [5–7].

In weak disorder, AL is due to the interference of waves multiply scattered from random defects, which results in absence of diffusion and spatially localized wavefunctions [8]. The paradigmatic signature of AL is obtained from the average logarithm of the transmission of a wave of energy E through a disordered region. In 1D, it is a self-averaging quantity characterized by the exponential decay $\overline{\ln|\psi_E(z)|^2} \simeq -2\gamma(E)|z|$, with $\gamma(E)$ the Lyapunov exponent (inverse localization length) [9]. The localization of a wave packet is a more complicated issue as it is determined by the superposition of many energy components. Since the latter cannot be separated from each other, the relevant quantity is rather the average of the localized density profile, $n(z) = \overline{|\psi(z)|^2}$, which is not self-averaging [9]. Moreover, each energy component localizes exponentially with its own localization length, and the superposition of all their contributions can lead to non-exponentially decaying density profiles [5, 10].

Localization of wave packets is for instance relevant to experiments where a Bose-Einstein condensate (BEC) propagates in a disordered potential [3]. The situation is modeled by the following scenario [5, 11]: A non-disordered, interacting BEC (with initial healing length $\xi_{\rm in}$) is first released from a trap. It expands in free space and its initial interaction energy is converted into kinetic energy. At a given time $t_{\rm i}$, a speckle potential (with correlation length $\sigma_{\rm R}$) is switched on and the interactions off. This creates a wave packet with a broad energy distribution. The energy components are then independent and eventually localize exponentially in the disordered potential, which results in the localization of the matter wave. For $\xi_{\rm in} > \sigma_{\rm R}$, recent experiments report an exponential decay of the density profile, in fair agreement with the prediction of the above scenario [3, 12]. The data however suggest deviations from exponential decay in the wings, the origin of which remains to be elucidated.

Here, we revisit the theoretical model for AL of matter wave packets in 1D disorder. Beyond previous models, our approach allows us to include (i) the phase-space density of the matter wave at time $t_{\rm i}$, and (ii) the spectral broadening induced by the disorder. We show that these ingredients significantly affect the predicted density profile of the localized matter wave at both short and long distances. It predicts a complex behavior of the density profile, which significantly deviate from pure exponential decay. Our results are confirmed by large-scale and long-time numerical calculations. They shed new light on the AL of matter wave packets, in particular on the experiments of Refs. [3, 12].

We consider a 1D matter wave subjected to a harmonic trap and a disordered potential, with repulsive short-range interactions. In the weakly interacting regime (i.e. for large enough 1D density, $n \gg mg/\hbar^2$, where m is the atomic mass and g is the coupling parameter), its dynamics is governed by the Gross-Pitaevskii equation,

$$i\hbar\partial_t\psi = \left[-(\hbar^2/2m)\partial_z^2 + V_{\rm ho}(z) + V(z) + g|\psi|^2 - \mu\right]\psi, \quad (1)$$

where μ is the chemical potential, the wavefunction is normalized to the total number of atoms ($\int {\rm d}z|\psi|^2 = N$), $V_{\rm ho}(z) = m\omega^2 z^2/2$ is the trapping potential, and $V(z)$ is the disordered potential. The latter is assumed to be stationary with a null ensemble average, $\overline{V} = 0$. It is characterized by the correlation function $C(z) = \overline{V(z')V(z'+z)}$. Hereafter, the quantities $V_{\rm R}$ and $\sigma_{\rm R}$ denote the amplitude and correlation length of the disorder (see below for precise definitions). We define the healing length of the trapped BEC by $\xi_{\rm in} \equiv \hbar/\sqrt{4m\mu}$. In the following, we study the average density profile: $n(z,t) = \overline{{\rm Tr}[\hat\rho(t)\hat n(z)]}$, with $\hat\rho$, the one-body density matrix and $\hat n(z) = \delta(z-\hat z)$, the spatial density operator.

Following the scenario of Refs. [5, 11], an interact-

ing BEC is first produced in the harmonic trap and in the absence of disorder. For interactions strong enough that $n \gg \hbar\omega/g$ [Thomas-Fermi regime (TF)], the phase is uniform and the density profile is a truncated inverted parabola, $n_0(z) = (\mu/g)[1-(z/L_{\rm TF})^2]_\oplus$, where $L_{\rm TF} = \sqrt{2\mu/m\omega^2}$ and $[f(z)]_\oplus = f(z)$ for $f(z) > 0$ and 0 otherwise. Then, an expanding matter wave is produced by switching off the trap ($V_{\rm ho} \to 0$) at time $t = 0$. We assume that, in the first expansion stage ($0 \leq t \leq t_{\rm i}$), the disordered potential is still off, so that the density matrix at time $t_{\rm i}$ is pure state: $\hat{\rho}(t_{\rm i}) = |\psi_{\rm i}\rangle\langle\psi_{\rm i}|$, where $\psi_{\rm i}(z) = {\rm e}^{{\rm i}\theta_{\rm i}(z)}\sqrt{n_{\rm i}(z)}$ is determined by the integration of Eq. (1) with $V \equiv 0$. The solution reads [13]

$$n_{\rm i}(z) = n_0\big(z/b(t_{\rm i})\big)/b(t_{\rm i}) \quad \text{and} \quad \theta_{\rm i}(z) = mz^2\dot{b}(t_{\rm i})/2\hbar b(t_{\rm i}), \tag{2}$$

where the scaling parameter is the unique solution of $\sqrt{b(t)[b(t)-1]} + \ln[\sqrt{b(t)} + \sqrt{b(t)-1}] = \sqrt{2}\omega t$ [14]. For $t \gg 1/\omega$, we have $b(t) \simeq \sqrt{2}\omega t + (1/2)[1 - \ln(4\sqrt{2}\omega t)]$.

The second expansion stage ($t > t_{\rm i}$) starts when the disorder is suddenly switched on and the interactions off ($V \not\equiv 0$ and $g \to 0$). Then, Eq. (1) reduces to the linear Schrödinger equation of Hamiltonian $\hat{H} = -\hbar^2\partial_z^2/2m + V(z)$ with the initial state given by Eq. (2) at time $t_{\rm i}$. Turning to the Heisenberg picture, we get:

$$n(z,t) = \overline{{\rm Tr}[\hat{\rho}(t_{\rm i})\hat{n}(z, t-t_{\rm i})]}. \tag{3}$$

We now treat the *initial* state of the second expansion stage semiclassically and apply the substitution $\hat{\rho}(t_{\rm i}) \to \int dz dE\ \delta(z-\hat{z})\mathcal{N}(E)^{-1} f_{\rm i}(z,E)\delta(E-\hat{H})$, where $\mathcal{N}(E)$ is the density of states per unit length associated to the Hamiltonian $\hat{H}$ above and $f_{\rm i}(z,E)$ represents the probability density to find an atom at position z with energy E [15]. Inspection of Eq. (2) legitimizes the semi-classical approximation: The initial state is characterized by the velocity field $v_{\rm i}(z) \equiv (\hbar/m)\partial_z\theta_{\rm i} = z\dot{b}(t_{\rm i})/b(t_{\rm i})$, associated to the local de Broglie wavelength $\lambda_{\rm dB}(z) \equiv \hbar/mv_{\rm i}(z) \sim \hbar t_{\rm i}/mz$ for $t_{\rm i} \gg 1/\omega$, and we find $\lambda_{\rm dB}(z) \ll n_{\rm i}/|\partial_z n_{\rm i}|$, except in a small region of width $\Delta z \sim \xi_{\rm in}$ near the edges of the BEC. For $t_{\rm i} \gg 1/\omega$, we can then use the phase-space distribution $W_{\rm i}(z,p) \simeq n_{\rm i}(z) \times \delta\big(p - mv_{\rm i}(z)\big)$, i.e.

$$W_{\rm i}(z,p) \simeq \mathcal{D}_{\rm i}(p) \times \delta\big[z - \big(b(t_{\rm i})/m\dot{b}(t_{\rm i})\big)p\big] \tag{4}$$

where $\mathcal{D}_{\rm i}(p) = \big(3N/4p_{\rm m}(t_{\rm i})\big)\ [1-(p/p_{\rm m}(t_{\rm i}))^2]_\oplus$ is the momentum distribution, with $p_{\rm m}(t_{\rm i}) \equiv (\hbar/\xi_{\rm in})(\dot{b}(t_{\rm i})/\sqrt{2}\omega)$ [16]. Averaging over the disorder, we can then write $\overline{f_{\rm i}(z,E)} \simeq \int dp\ W_{\rm i}(z,p)A(p,E)$, where $A(p,E) = -{\rm Im}\langle p|\overline{G}(E)|p\rangle/\pi$ is the spectral function, which represents the probability density that a particle in the state of momentum p, $|p\rangle$, has energy E in the disorder. Here, $G(E) = [E - \hat{H} + {\rm i}0^+]^{-1}$ is the retarded Green operator associated to Hamiltonian $\hat{H}$ at energy E [10]. In order to evaluate the BEC density, we finally insert these formulas into the rhs term of Eq. (3) [17], which yields

$$n(z,t) = \int dz_{\rm i} dE \int dp\ W_{\rm i}(z_{\rm i},p)A(p,E)P(z-z_{\rm i}, t-t_{\rm i}|E) \tag{5}$$

with $P(z-z_{\rm i},\tau|E) \equiv \mathcal{N}(E)^{-1}\overline{{\rm Tr}[\delta(E-\hat{H})\hat{n}(z,\tau)\delta(z_{\rm i}-\hat{z})]}$. The quantity $P(z-z_{\rm i}, t-t_{\rm i}|E)$ is interpreted as the probability of quantum diffusion, that is the probability density to find in z at time t, a particle of energy E that was located in $z_{\rm i}$ at time $t_{\rm i}$ [18].

Equation (5) allows us to determine the density profile of the matter wave packet. Our approach goes beyond that of Ref. [5]. It allows us to take into account (i) the initial position distribution and (ii) the spectral broadening $A(p,E)$ of a particle of momentum p in the disordered potential [19]. We will show below that both play a significant role in the localization process.

In order to calculate the average spectral function, we solve the Dyson equation, $\overline{G} = G_0 + G_0\Sigma\overline{G}$, where $G_0(E) = [E - \hat{p}^2/2m + {\rm i}0^+]^{-1}$ is the free Green operator and $\Sigma(E) = \Sigma'(E) + {\rm i}\Sigma''(E)$ is the self-energy, both in the retarded form. For $V_{\rm R}^2 \ll E^{3/2}E_{\rm c}^{1/2}$ where $E_{\rm c} \equiv \hbar^2/2m\sigma_{\rm R}^2$ [i.e. $\gamma(E) \ll p_E/\hbar$], we find [20]

$$A(p,E) = \frac{(-1/\pi)\ \Sigma''(E,p)}{\big(E - p^2/2m - \Sigma'(E,p)\big)^2 + \Sigma''(E,p)^2} \tag{6}$$

with $\Sigma(E,p) \simeq \langle p|\overline{VG_0(E)V}|p\rangle$. Performing the integration, we get the explicit formula

$$\Sigma''(E,p) \simeq -(m/2\hbar p_E)\big\{\tilde{C}(p_E - p) + \tilde{C}(p_E + p)\big\} \tag{7}$$

where $\tilde{C}(p) \equiv \int dz\ C(z)\exp(-{\rm i}pz/\hbar)$ is the Fourier transform of the correlation function, and $p_E \equiv \sqrt{2mE}$ is the momentum associated to energy E in free space. The real-part of the self-energy, $\Sigma'(E,p) = \int \frac{dq}{2\pi\hbar}\tilde{C}(q-p) \times {\rm PV}\big(\frac{1}{E - q^2/2m}\big)$ with PV the Cauchy principal value, turns out to be negligible and we disregard it in the remainder of this work.

In order to calculate the probability of quantum diffusion, we rely on the diagrammatic method developed in Refs. [18, 21]. In the weak disorder limit ($\gamma(E) \ll \sigma_{\rm R}^{-1}, p_E/\hbar$), it provides the infinite-time limit [22]

$$P_\infty(z|E) = \frac{\pi^2\gamma(E)}{8}\int_0^\infty {\rm d}u\ u\ \sinh(\pi u)\left[\frac{1+u^2}{1+\cosh(\pi u)}\right]^2 \times \exp\big\{-(1+u^2)\gamma(E)|z|/2\big\} \tag{8}$$

with the Lyapunov exponent

$$\gamma(E) \simeq (m^2/2\hbar^2 p_E^2)\ \tilde{C}(2p_E). \tag{9}$$

We now compare the predictions of our analytical model to the results of numerical calculations. In order to integrate Eq. (1), we use a Crank-Nicolson algorithm, with space step $\Delta z = 0.1\sigma_{\rm R}$ and time step $\Delta t = 0.05\hbar/E_{\rm c}$, in a box with Dirichlet boundary conditions [23]. The disorder is a 1D speckle potential, which can be written in the form $V(z) = V_{\rm R} \times \{v(z) - \overline{v}\}$, where $v(z) \geq 0$ represents the speckle intensity pattern and the sign of $V_{\rm R}$ depends on the detuning of the laser light with respect to the atomic resonance: $V_{\rm R} > 0$ for blue detuning, and $V_{\rm R} < 0$ for red detuning [24, 25]. We use

parameters close to those of Ref. [3] and both blue and red detunings ($V_{\rm R} = \pm 0.0325 E_{\rm c}$). In both cases, the correlation function reads

$$\tilde{C}(p) = \pi V_{\rm R}^2 \sigma_{\rm R} [1 - |p|\sigma_{\rm R}/2\hbar]_{\oplus}, \qquad (10)$$

in Fourier space. Our numerical calculations differ from those of Ref. [5] in that we use significantly larger boxes and longer times. Moreover, we consider here exactly the above scenario where the disorder is switched on and the interactions off at a time $t_{\rm i} \gg 1/\omega$, while in the numerics of Ref. [5], both disorder and interactions were on during the whole expansion. Due to the cutoffs of $\tilde{C}(p)$ at $p = \pm 2\hbar/\sigma_{\rm R}$, the quantities $\gamma(E)$ and $P_\infty(z|E)$ vanish for $E > E_{\rm c}$ and it is useful to distinguish two cases for the analysis of the density profiles.

Case $2\mu < E_c$ (i.e. $\xi_{in} > \sigma_R$) - The left panel of Fig. 1 shows the time evolution of the density profile in semi-logarithmic scale for $\xi_{\rm in} > \sigma_{\rm R}$. For $t < t_{\rm i} \equiv 10/\omega$ [Fig. 1(a1)], the matter wave expands in free space, with the shape of a truncated inverted parabola of increasing size, according to Eq. (2). When the disorder is switched on and the interactions off, the matter wave continues expanding and develops long wings [Fig. 1(a2)]. In the long-time limit [Fig. 1(a3)], the density profile converges to a stationary shape, hence demonstrating AL. The localized density profile is in fair agreement with the theoretical prediction based on Eq. (5), using Eqs. (4), (6) and (8) for the correlation function (10), with a global multiplying factor as the only fitting parameter [see the solid black line in Fig. 1(a3)]. This holds over the full space, except very close to the center. There, for the chosen parameters, Eq. (5) predicts a nonphysical dip due to the overestimation of the Lyapunov exponents and the spectral broadenings at low energies in the lowest-order perturbation theory used to derive Eqs. (6) and (8). This dip affects the balance between the center and the wings in the normalization of the wavefunction, which justifies the multiplying factor to correctly fit the wings. These results validate the localization model of the matter wave.

Let us now discuss the density profile in more detail, and accordingly examine the impact of the various terms in Eq. (5). For $|z| \lesssim b(t_{\rm i}) L_{\rm TF}$, the stationary density profile is mainly determined by particles originating from the BEC at time $t_{\rm i}$ that propagate over very short distances in the disordered potential. Using the full phase-space distribution $W_{\rm i}(z,p)$ is then necessary to account for the central feature of the density profile. For $|z| \gtrsim b(t_{\rm i}) L_{\rm TF}$ only, we can neglect the initial density distribution and rely on the approximation $W_{\rm i}(z,p) \to \mathcal{D}(p) \times \delta(z)$ in Eq. (5). For $b(t_{\rm i}) L_{\rm TF} \lesssim |z| \lesssim 1/2\gamma(2\mu)$, we find that the density profile shows an essentially exponential decay of rate approximately equal to $2\gamma(2\mu)$ [see the dashed green line in Fig. 1(a3)]. This is consistent with experimental observations [3]. For longer distances however, the logarithmic derivative of the density continuously decreases in modulus. Neglecting the spectral broadening induced by the disorder [5, 11], $A(p,E) \to \delta(E - p^2/2m)$, we are able to reproduce the numerical results over about five decades [see the dotted black line in Fig. 1(a3)]. This approximation cuts all components with $E > 2\mu$ and predicts a long-distance exponential decay of rate $\gamma(2\mu)/2$ [5, 22]. This behavior can be understood on the basis of the probability of quantum diffusion (8), which continuously interpolates from $d \ln P_\infty(z|E)/dz \simeq -2\gamma(E)$ for $|z| \ll 1/2\gamma(E)$ to $d \ln P_\infty(z|E)/dz \simeq -\gamma(E)/2$ for $|z| \gg 2/\gamma(E)$ [21]. For $|z| \gg 2/\gamma(2\mu)$, the numerics show significant deviation from exponential decay, owing to the Lorentzian-like form of the spectral function (6) which populates components with $E > 2\mu$. Then, taking into account the full spectral function, Eq. (5) fits the numerics well [see the solid black line in Fig. 1(a3)]. Finally, note that our model relies on the Born approximation which is not sufficient to account for components with $E > E_{\rm c}$ [6]. To do so, it would be necessary to include arbitrary high-order terms at arbitrary large distances. It however appears irrelevant in the space window used for the numerics.

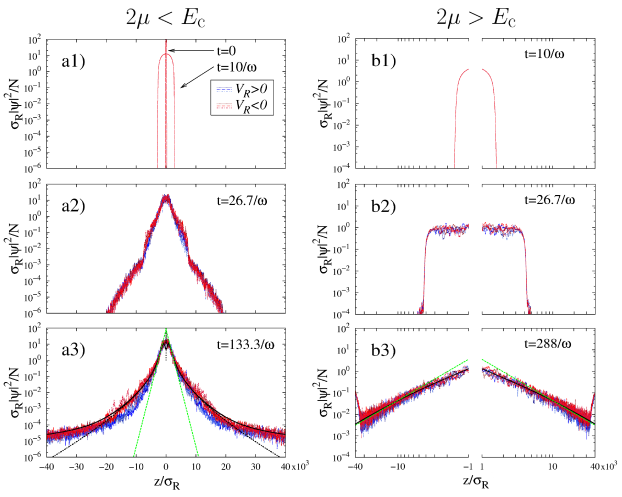

Figure 1. (color online) Time evolution of the density profile of a matter wave expanding in 1D speckle potentials for $2\mu < E_{\rm c}$ (left panel) and $2\mu > E_{\rm c}$ (right panel). Shown are the running averages, $\tilde{n}(z) = \int_{-l/2}^{+l/2} \frac{dx}{l} n(z+x)$ with $l = 100\sigma_{\rm R}$, of numerical data, for blue- and red-detuned speckle potentials (three realizations each) [23]. Here, we use $\omega = 2 \times 10^{-2} \mu/\hbar$ and $V_{\rm R} = \pm 0.0325 E_{\rm c}$. Left panel [(a1)-(a3)]: semi-logarithmic scale for $\xi_{\rm in} = 1.5\sigma_{\rm R}$ ($2\mu \simeq 0.44 E_{\rm c}$). The solid black line shows a fit of the full Eq. (5) and the dotted black line to Eq. (5) with $A(p,E) \to \delta(E - p^2/2m)$, both with a multiplying factor as the only fitting parameter. The dashed green line is a fit of $\ln[n(z)] = A - 2\gamma(2\mu)|z|$, with A as the fitting parameter. Right panel [(b1)-(b3)]: log-log scale for $\xi_{\rm in} = 0.83\sigma_{\rm R}$ ($2\mu \simeq 1.44 E_{\rm c}$). The solid black line shows the full Eq. (5) and the dashed green line is a fit of $n(z) = A/|z|^\beta$ with A and β as the fitting parameters.

Case $2\mu > E_c$ (i.e. $\xi_{in} < \sigma_R$) - The right panel of Fig. 1 shows the counterpart of the left panel for $\xi_{\rm in} < \sigma_{\rm R}$ and in log-log scale. In this regime too, the complete model of Eq. (5) reproduces well the numerical results over the full space (except very close to the center), with

a multiplying factor as the only fitting parameter [see the solid black line in Fig. 1(b3)]. In 1D speckle potentials, the correlation function provides a high-momentum cutoff which strongly suppresses backscattering of matter waves with momentum $p > \hbar/\sigma_{\rm R}$ [5, 6]. For $E > E_{\rm c}$, the Lyapunov exponent, calculated in the Born approximation then vanishes [see Eq. (9)], and the determination of $P_\infty(z|E)$ would require an extension of the formalism of Refs. [18, 21] by at least two orders in perturbation theory. Using the results of Refs. [6] based on the phase-formalism approach, we estimate that, for our parameters, the Lyapunov exponent drops by about two orders of magnitude around $E \simeq E_{\rm c}$ and we neglect localization of waves with $E > E_{\rm c}$. Since $E_{\rm c} < 2\mu$, the spectral broadening has little importance here and we can safely rely on the approximation $A(p, E) \to \delta(E–p^2/2m)$. The above model then predicts algebraic localization, $n(z) \propto 1/|z|^2$ [5]. Fitting an algebraic function, $A/|z|^\beta$ with A and β as fitting parameters, to the numerical data of three different realizations of blue- and red-detuned speckle potentials in the intervals $[-30, -10]$ and $[+10, +30]$ independently, we find $\beta \simeq 1.91 \pm 0.22$. This is in fair agreement with the analytical prediction (within the error bars) and was observed in Ref. [3].

In summary, we have developed a theoretical model for the AL of a matter wave packet with initial healing length $\xi_{\rm in}$ in a 1D speckle potential with correlation length $\sigma_{\rm R}$. It extends previous approaches by including (i) the initial phase-space density of the matter wave, and (ii) the spectral broadening induced by the disorder. We have shown that these ingredients affect the localized density profiles, which significantly deviate from a pure exponential decay. For $2\mu < E_{\rm c}$, we found that $n(z)$ essentially shows an exponential decay of rate $2\gamma(2\mu)$ at short distance, in accordance with experimental observations [3]. For larger distance, $n(z)$ crosses over to an exponential decay of rate $\gamma(2\mu)/2$ and then deviates from exponential decay due to the disorder-induced spectral broadening. This may explain the very large distance behavior of experimental data [3, 12]. For $2\mu > E_{\rm c}$, we found algebraic localization, $n(z) \propto 1/|z|^2$, as observed in Ref. [3].

In the future, it would be interesting to extend the present approach toward two directions. First, our analysis relies on the calculation of the probability of quantum diffusion, $P_\infty(z|E)$, to lowest order, which is valid only below the effective mobility edge at $E = E_{\rm c}$ [6]. Extending the diagrammatic method of Refs. [18, 21] to higher orders would allow one to incorporate the components of energy $E > E_{\rm c}$. In addition, it may explain the slight difference in the localized density profiles found for blue- and red-detuned speckle potentials [see Fig. 1(a3)]. Second, although ultracold atoms allow for an exact realization of the above scenario using time-dependent control of optical disorder and of interactions via Feshbach resonance techniques, recent experiments have followed a slightly different scheme where the BEC is created already in the presence of the disorder and the interactions are not switched off [3, 12]. Extending our model to this case would require one to include (i) the effect of the disorder at $t \lesssim 1/\omega$, which can significantly modify the relevant phase-space density $W_{\rm i}(z, p)$ and (ii) the effect of interactions in the probability of quantum diffusion $P_\infty(z|E)$. Whether and how interactions destroy localization in this scheme is still a very debated subject [26].

We thank Peter Schlagheck, Luca Pezzé, Dominique Delande, Georgy Shlyapnikov and Randy Hulet for stimulating discussions. This research was supported by the European Research Council (FP7/2007-2013 Grant Agreement No. 256294), Agence Nationale de la Recherche (ANR-08-blan-0016-01), Ministère de l'Enseignement Supérieur et de la Recherche, Triangle de la Physique and Institut Francilien de Recherche sur les Atomes Froids (IFRAF). We acknowledge GMPCS high performance computing facilities of the LUMAT federation.

[1] A. Lagendijk, B.A. van Tiggelen, and D.S. Wiersma, Phys. Today **62**, 24 (2009); A. Aspect, and M. Inguscio, Phys. Today **62**, 30 (2009).
[2] L. Sanchez-Palencia and M. Lewenstein, Nature Phys. **6**, 87 (2010); L. Fallani, C. Fort, and M. Inguscio, Adv. At. Mol. Opt. Phys. **56**, 119 (2008).
[3] J. Billy *et al.*, Nature (London) **453**, 891 (2008).
[4] G. Roati *et al.*, Nature (London) **453**, 895 (2008).
[5] L. Sanchez-Palencia, *et al.*, Phys. Rev. Lett. **98**, 210401 (2007); New J. Phys. **10**, 045019 (2008).
[6] E. Gurevich and O. Kenneth, Phys. Rev. A **79**, 063617 (2009); P. Lugan *et al.*, Phys. Rev. A **80**, 023605 (2009).
[7] L. Pezzé and L. Sanchez-Palencia, Phys. Rev. Lett., **106**, 040601 (2011).
[8] P.A. Lee and T.V. Ramakrishnan, Rev. Mod. Phys. **57**, 287 (1985); M. Janssen, Phys. Rep. **295**, 1 (1998).
[9] I.M. Lifshits, S.A. Gredeskul, and L.A. Pastur, *Introduction to the Theory of Disordered Systems* (Wiley, New York, 1988).
[10] S.E. Skipetrov, A. Minguzzi, B.A. van Tiggelen, B. Shapiro, Phys. Rev. Lett. **100**, 165301 (2008).
[11] B. Shapiro, Phys. Rev. Lett. **99**, 060602 (2007).
[12] R. Hulet *et al.*, private communication.
[13] Yu. Kagan, E.L. Surkov, and G.V. Shlyapnikov, Phys. Rev. A **54**, R1753 (1996): Y. Castin and R. Dum, Phys. Rev. Lett. **77**, 5315 (1996).
[14] D. Clément *et al.*, Phys. Rev. Lett. **95**, 170409 (2005).
[15] We may use alternative semi-classical approaches. For instance, the Wigner distribution provides similar results. In fact, Eq. (4) accurately approximates the latter.
[16] In the long-time limit ($t_{\rm i} \to \infty$), we find $p_{\rm m} \to \hbar/\xi_{\rm in}$.
[17] This approach neglects possible correlations in disorder-averaging of the initial state and the propagation kernel. For weak disorder, it is reasonable to assume they are small, which is supported by the good agreement between Eq. (5) and numerical calculations (see text).

[18] V.L. Berezinskii, Sov. Phys. JETP **38**, 620 (1974).
[19] We recover the formulation of Ref. [5] by using the substitutions $W_{\rm i}(z,p) \to \mathcal{D}(p) \times \delta(z)$, which holds at distances exceeding the initial size of the gas, and $A(p,E) \to \delta(E-p^2/2m)$, which is the free spectral function.
[20] J. Rammer, *Quantum Transport Theory* (Westview press, Boulder, CO, 2004).
[21] A.A. Gogolin, V.I. Mel'nikov, and E.I. Rashba, Sov. Phys. JETP **42**, 168 (1976); A.A. Gogolin, Sov. Phys. JETP **44**, 1003 (1976).
[22] In Ref. [5], the term inside the exponential function in $P_\infty(z|E)$ was mistakenly written [see erratum to Ref. [5], to be published]. The present Eq. (8) is the correct formula.
[23] Only the central half of the box used in the numerics is plotted in Fig. 1. We have checked that the boundary conditions do not significantly alter the results in the represented space window by using boxes of different sizes.
[24] J.W. Goodman, *Speckle Phenomena in Optics: Theory and Applications* (Roberts & Company publishers, Englewood, Colorado, 2007).
[25] D. Clément *et al.*, New J. Phys. **8**, 165 (2006).
[26] A.S. Pikovsky and D.L. Shepelyansky, Phys. Rev. Lett. **100**, 094101 (2008); G. Kopidakis, S. Komineas, S. Flach, and S. Aubry, Phys. Rev. Lett. **100**, 084103 (2008); S. Palpacelli and S. Succi, Phys. Rev. E **77**, 066708 (2008); S. Flach, D.O. Krimer, and C. Skokos, Phys. Rev. Lett. **102**, 024101 (2009).